Trees (2016) 30:1683–1693
DOI 10.1007/s00468-016-1400-y

ORIGINAL ARTICLE

Influence of the exclusion distance among trees on gap fraction and foliage clumping index of forest plantations

Jun Geng[1] · Jing-Ming Chen[1,3] · Li-Li Tu[1,2] · Qing-Jiu Tian[1,2] · Lei Wang[1,2] · Ran-Ran Yang[1,2] · Yan-Jun Yang[1,2] · Yan Huang[1,2] · Wei-Liang Fan[4,5] · Chun-Guang Lv[1,2] · Guang Zheng[1,2]

Received: 28 October 2015 / Accepted: 15 April 2016 / Published online: 20 June 2016

Abstract

Key message **A hypergeometric model is proposed explicitly instead of two previous stochastic models (the Poisson model and Neyman-A model) to describe the topological relationship of trees and the influence of the exclusion distance on gap fraction and clumping index of forest plantation canopies.**

Abstract Gap fraction (GF) and clumping index (CI) play key roles in plant light interception, and therefore they have strong impacts on plant growth and canopy radiative transfer processes. Trees are usually assumed to be randomly distributed in natural forests in many previous studies. However, few studies have shown how trees are distributed in forest plantations and how these distribution patterns affect GF and CI in these forests. In this paper, a simple and general distance factor defined as relative allowable shortest distance between centers of two adjacent crowns divided by the mean diameter of the crowns (RASD) is proposed to describe quantitatively the degree of mutual exclusion among trees in forest plantations of various tree distribution patterns. A hypergeometric model is proposed instead of two previous stochastic tree distribution models (the Poisson model and Neyman-A model) to describe the topological relationship of trees and the influences of the exclusion distance on the GF and CI of the forest plantation canopies. The results show that: (1) the hypergeometric model is more suitable than the Poisson model and Neyman-A model for describing the topological relationship of trees in forest plantations; (2) the exclusion distance has strong impacts on GF and CI: there are significant differences between the results of the hypergeometric model and the Poisson model. Larger RASD causes lower GF and larger CI. The simulations are verified by field measurements in four forest plantation stands. Similarly, impacts of RASD on GF and CI are also found for other two crown shapes (prolate and oblate ellipsoids).

Keywords Forest plantations · Exclusion distance · Hypergeometric distribution model · Gap fraction · Clumping index

Communicated by R. Matyssek.

✉ Qing-Jiu Tian
tianqj@nju.edu.cn

[1] International Institute for Earth System Sciences, Nanjing University, Nanjing 210023, China

[2] Jiangsu Provincial Key Laboratory of Geographic Information Science and Technology, Nanjing University, Nanjing 210023, China

[3] Department of Geography, University of Toronto, 100 St. George Street, Toronto, ON M5S 3G3, Canada

[4] State Key Laboratory of Remote Sensing Science, Institute of Remote Sensing and Digital Earth, Chinese Academy of Sciences, Beijing 100101, China

[5] University of Chinese Academy of Sciences, Beijing 100049, China

Introduction

Plant canopy structure exerts a major influence on the radiation regime within the canopy. In forests, the structure of the tree overstory influences not only radiation absorption by the trees for photosynthesis and energy exchange with the atmosphere (Ross 1981) but also radiation transmission to the understory and the soil surface that has various physical and ecological significance in the forest ecosystem (Niinemets 2010; Duursma et al. 2012; Xue et al. 2011). These canopy structural effects are often

quantified using canopy gap fraction (GF) and clumping index (CI). These parameters are closely related to the light interception or capture by the canopies, and therefore they are very important for understanding the radiative transfer and physiological processes in the canopies (Massonnet et al. 2008; Talbot and Dupraz 2012; Yang et al. 2015). GF, also known as gap frequency or gap probability, is defined as the probability of a ray of light passing through the canopy without encountering foliage or other plant elements (Li and Strahler 1988). It can be expressed using the well-known Lambert–Beer model as:

$$P(\theta) = \exp[-k \times L/\cos\theta] \quad (1)$$

where $P(\theta)$ is GF at solar zenith angle θ, k is the projection coefficient quantifying projection of foliage area on a plane perpendicular to θ, and L is the leaf area index (LAI) defined as one half the total leaf area per unit horizontally projected ground surface area (Chen and Black 1992; Duursma and Makela 2007). The Lambert–Beer model assumed that light-intercepting objects are randomly distributed in space. However, the spatial random distribution of leaves is clearly a poor assumption for most forest canopies. For this reason, a leaf dispersion parameter is frequently introduced as:

$$P(\theta) = \exp[-k \times L \times \Omega/\cos\theta] \quad (2)$$

where the dispersion parameter Ω is often referred to as CI, which is defined as the ratio of the effective LAI to the true LAI, and is an important vegetation structure parameter to quantify the influence of the spatial agglomeration of leaves or shoots on radiation transmission through the canopy (Chen and Cihlar 1995; Nilson 1971). CI is useful in many ecological models because it provides new information in addition to the effective LAI retrieved from remote sensing and allows accurate separation of sunlit and shaded leaves in the canopy (Chen et al. 1999, 2005).

GF and CI have been studied at many scales, i.e., sub-crown, crown, and stand as well as mapped at regional and global scales using remote sensing data (Chen et al. 2005; Demarez et al. 2008; He et al. 2012; Iio et al. 2009; Mottus et al. 2006; Nelson et al. 2014). At the crown or sub-crown scale, the methods of three-dimensional (3-D) architectural simulations were usually used to calculate GF and CI by modeling the organization of leaves in canopies (Da Silva et al. 2014; Lewis and Disney 2007; Munier-Jolain et al. 2013; Sinoquet et al. 2007; Zheng et al. 2013). However, reconstruction of detailed canopy architecture in a computer is still very labor-intensive and time-consuming. At the stand level, GF and CI have been extensively modeled based on various tree distribution models in the field of remote sensing (Chen and Leblanc 1997; Li and Strahler 1988; Nilson et al. 2011). These models usually describe plant structural parameters (i.e., the spatial positions of crowns) to meet a specific probability distribution. Therefore, they have a much higher execution speed than 3-D architectural simulations, and they can also guarantee certain accuracy reliable for a wide range of applications. For example, the Poisson model was used to describe the spatial relationship of trees in early geometric-optical models for natural forest canopies (Li and Strahler 1988). The influences of clumped tree distributions (Franklin et al. 1985) on radiative transfer in natural forests have been previously considered using the Neyman-A type distribution (also called the double-Poisson distribution) (Chen and Leblanc 1997; Franklin et al. 1985).

The above-mentioned studies are all focused on natural forests. However, few studies have shown how trees are distributed in forest plantations which tend to have regular tree distribution patterns due to human influence, and how these distribution patterns affect GF and CI. Although the exclusion effect had been considered in the five-scale geometric-optical model for forest canopies (Leblanc et al. 1999), the exclusion distance was a prescribed value and not described explicitly according to the specific geometry of crowns. China has 6.9×10^{12} m^2 forest plantations, which is about one-third of the total forest plantations in the world according to the eighth national forest resources inventory of China. Therefore, it is necessary to study tree distribution patterns in forest plantations and influences of these patterns on GF and CI. The aims of the paper are to: (1) define a simple and general exclusion distance factor for quantifying the degree of the mutual exclusion among trees in forest plantations; (2) develop a statistical tree distribution model suitable for forest plantations at the stand level; (3) exhibit how tree distribution patterns impact GF and CI in forest plantations.

Theory and methods

Stochastic tree distribution models for natural forests

The Poisson model

The Poisson model is a common tree distribution model to express topological or spatial relationships of trees in natural forests in the fields of tree physiology, forest ecology and remote sensing (Franklin et al. 1985; Russell et al. 1989; Li and Strahler 1988). Based on the hypothesis of random distribution of natural resources, the Poisson model assumed that trees are completely randomly distributed in natural forests. Then GF of a forest can be calculated using the Poisson model as

$$P_{\mathrm{P}\_t}(\theta) = \sum_{i=0}^{N_c} P_{\mathrm{P}}(i) \times \left[1 - \frac{t_c(\theta) \times (1 - P_c(\theta))}{S \times \cos(\theta)}\right]^i \quad (3)$$

where $P_{\mathrm{P}\_t}(\theta)$ is GF of the Poisson model, N_c is the total number of trees in the forest, and S is the area of the forest. $P_{\mathrm{P}}(i)$ represents the Poisson probability of finding i trees in a quadrat (a forest is divided into a number of equal-sized quadrats), $t_c(\theta)$ is the projected area of a crown at θ, and $P_c(\theta)$ is the GF of an individual crown at θ (Chen and Leblanc 1997; Fan et al. 2014a, b), and it can be calculated as

$$P_c(\theta) = e^{-G(\theta) \times L \times S \times \Omega_C(\theta)/(N_c \times t_c(\theta) \times \gamma_e)} \quad (4)$$

where $G(\theta)$ is the projection of unit leaf area and is equal to 0.5 for the spherical leaf angular distribution inside the crown. $\Omega_C(\theta)$ is the CI for leaves or shoots in an individual crown (CIc) at θ. γ_e is the ratio of half total needle area in a shoot to half total shoot surface area for coniferous forests, and is equal to 1 for broad-leaved forests (Chen and Leblanc 1997).

The Neyman-A distribution (double-Poisson model)

Variations in environmental conditions often make the tree spatial distributions non-random, i.e., trees in a forest are often grouped to form patches or communities due to topographical variations and uneven soil distributions. For this reason, the Poisson model is incapable of describing such patchiness or community effect in natural forests.

The Neyman distribution assumes that trees are randomly distributed in communities or groups with equal area first, and then the center of each community is distributed according to the Poisson model (Neyman 1939). This model called the Neyman-A or double-Poisson model by Franklin et al. (Franklin et al. 1985). Then GF of a canopy becomes

$$P_{\mathrm{N}\_t}(\theta) = \sum_{i=0}^{k} P_{\mathrm{N}}(i) \times \left[1 - \frac{t_c(\theta) \times (1 - P_c(\theta))}{S \times \cos(\theta)}\right]^i \quad (5)$$

where $P_{\mathrm{N}\_t}(\theta)$ is GF of the Neyman-A model, $P_{\mathrm{N}}(i)$ is the Neyman-A probability of having i trees in a quadrat, and k is an integer which should be large enough to consider all overlapping of the trees in a quadrat (Chen and Leblanc 1997).

A hypergeometric distribution model for forest plantations

Forest plantations are usually affected by humans to form more regular tree distribution patterns than natural forests. Trees in forest plantations at the stand level hardly completely overlap each other, so that every tree can more or less have equal opportunities to intercept light and to access to water and nutrients (West 2006). In other words, the exclusion distances among trees in forest plantations are larger than those in natural forests. These distances produce a "crust" or a buffer zone for every crown. Figure 1 shows tree positions in a sample plot of a forest plantation stand of *Pinus massoniana* in Chuzhou, China (32°33′00″N; 118°12′09″E). Measurements of tree positions and the radius of crowns were made by means of quadrate investigation in October 2013. Obvious exclusion distances among trees are found from Fig. 1. Therefore, considering the exclusion distances among trees, the tree distribution in a forest plantation stand often does not follow the Poisson model or Neyman-A model because the two models would predict considerable overlap among tree crowns, and therefore a hypergeometric model is developed to overcome this issue.

The hypergeometric model describes the probability of k successes in n draws, without replacement, from a finite population of size N that contains exactly m successes. Its probability mass function is given by

$$f(k; n, m, N) = \frac{\binom{m}{k}\binom{N-m}{n-k}}{\binom{N}{n}} \quad (6)$$

If $n = 1$, the hypergeometric distribution is the binomial distribution which is an independent event; while it is a conditional probability if $n > 1$, because every foregoing sampling result could affect the subsequent sampling probability. It means that every sampled object occupies a certain space and this space must be discounted after it is sampled for the subsequent sampling. The canopy GF can be calculated similarly as this event sampling without replacement. If trees are assumed to be solid spheres ($P_c(\theta) = 0$), the GF at $\theta = 0°$ can be calculated as: $(S - t_c)/S$ after the first tree is put on the ground; then GF become $(S - 2 \times t_c)/(S - t_c)$ after the second tree is put on the ground. After considering n trees, GF can be calculated as

$$\frac{S - t_c}{S} \times \frac{S - 2 \times t_c}{S - t_c} \times \frac{S - 3 \times t_c}{S - 2 \times t_c} \times \cdots \times \frac{S - n \times t_c}{S - (n-1) \times t_c} = \frac{S - n \times t_c}{S} \quad (7)$$

The main difference between GF in Eq. (7) and GF simulated by Poisson model (Eq. 3) is that in Eq. (7), the denominator decreases gradually as trees are added one by one, because every tree has its own space, and the total space for subsequent tree distribution is reduced after a tree is added. This process as described in Eq. (7) is sampling without replacement.

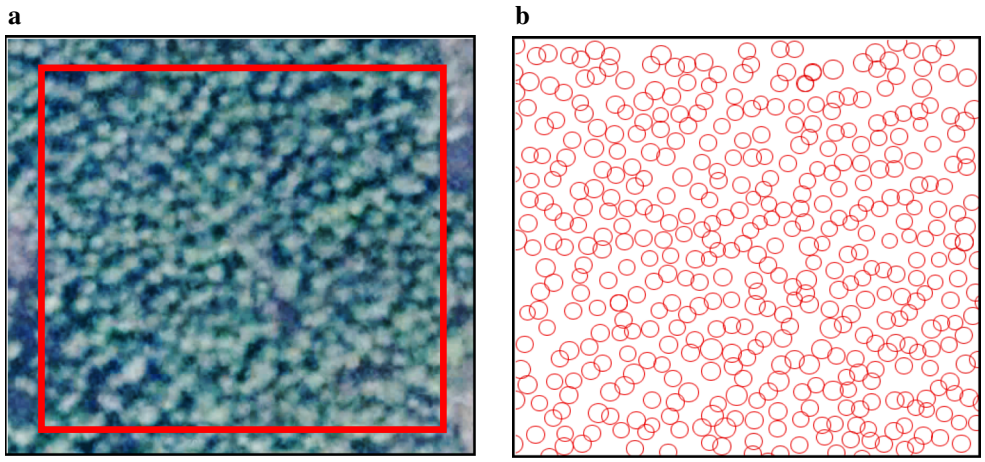

Fig. 1 Trees position in a 100 × 100 m^2 sample plot of *P. massoniana* plantation. **a** Obvious exclusion distances among trees are found in the plot from Google earth; *red rectangle* is the boundary of the plot; **b** measurements of trees position in the sample plot by means of quadrate investigation; the *red circles* represent crowns (about 425 crowns) (color figure online)

Trees are more complicated than the solid spheres in real forests. In our study, exclusion distances among trees in a forest plantation stand are described using a simple parameter called relative allowable shortest distance (RASD), which is defined as the relative allowable shortest distance between centers of two adjacent crowns divided by the mean diameter of the crowns. By definition, the Poisson model is a special case of the hypergeometric distribution model, i.e., the "RASD" of the Poisson model is equal to 0.

The hypergeometric probability of having i trees in a quadrat is

$$P_{\mathrm{H}}(i) = \sum_{i=0}^{n_{\mathrm{qc}}} \binom{N_{\mathrm{c}}}{i} \times P_{\mathrm{H1}}(i) \times P_{\mathrm{H2}}(i)/P_{\mathrm{H0}}(N_{\mathrm{c}}) \tag{8}$$

where n_{qc} is the maximum number of trees in a quadrat and it can be calculated as

$$n_{\mathrm{qc}} = \frac{S}{N_{\mathrm{q}} \times \pi \times (r \times R_{\mathrm{ASD}})^2} \tag{9}$$

where N_{q} is the number of quadrats in a stand, r is the mean radius of crowns, and R_{ASD} is RASD. $P_{\mathrm{H0}}(N_{\mathrm{c}})$ in Eq. (8) means that there are N_{c} trees in the stand and the trees meet the hypergeometric distribution. It can be calculated as

$$P_{\mathrm{H0}}(N_{\mathrm{c}}) = \prod_{j=0}^{N_{\mathrm{c}}} \left[1 - \frac{\pi \times (r \times R_{\mathrm{ASD}})^2}{S} (j-1) \right] \tag{10}$$

$P_{\mathrm{H1}}(i)$ in Eq. (8) means that there are i trees in a quadrat and the trees meet the hypergeometric distribution; $P_{\mathrm{H2}}(i)$ means that there are $N_{\mathrm{c}} - i$ trees outside the quadrat and the trees meet the hypergeometric distribution. They are calculated as

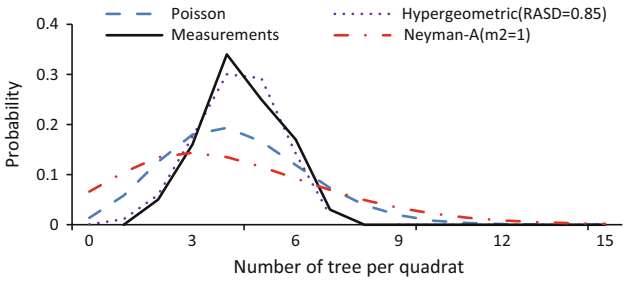

Fig. 2 The tree distribution in the plantation stand of *P. massoniana* divided in 100 quadrats compared with the Poisson, Neyman-A and hypergeometric distributions. (m_2 in the Neyman-A model means the average number of trees in a cluster. The minimum value of m_2 in the Neyman-A model is 1. The larger value of m_2 means stronger clumping of the trees and a broader line distribution)

$$P_{\mathrm{H1}}(i) = P_{\mathrm{H0}}(i) \times \left(1/N_{\mathrm{q}}\right)^i \tag{11}$$

$$P_{\mathrm{H2}}(i) = P_{\mathrm{H0}}(N_{\mathrm{c}} - i) \times \left(1 - 1/N_{\mathrm{q}}\right)^{N_{\mathrm{c}} - i} \tag{12}$$

where N_{q} is the number of quadrats in a forest stand.

The sample plot in Fig. 1 is divided equally into 100 quadrats, and the number of quadrats having a certain number of trees is shown in Fig. 2. The line of measurements is distributed narrowly around the mean number of trees per quadrat while the Poisson and the Neyman-A distributions are much broader. Measurements from the sample plot show an obvious deviation of the tree distribution from the Poisson and the Neyman-A random cases but a good consistency with the hypergeometric model with the RASD = 0.85.

A larger value of RASD means a larger exclusion distance among trees and a larger area of the crust for every crown. If the nearest two crowns are tangent to each other

at $\theta = 0$, the RASD is equal to 1; if the nearest two crowns are intercrossed at $\theta = 0$, then the RASD is less than 1 (Fig. 3a); the RASD is greater than 1, if the nearest two crowns are separated at $\theta = 0$ (Fig. 3b). Taking the spherical crowns for example, GF can be calculated using the hypergeometric model (similarly as Eq. 7):

$$P_{\mathrm{H}\_t}(\theta) = \sum_{i=1}^{n_{\mathrm{qc}}} P_{\mathrm{H}}(i) \times \prod_{\mathrm{j}=1}^{i} \times \left[1 - \frac{t_{\mathrm{c}}(\theta) \times (1 - P_{\mathrm{c}}(\theta))}{S \times \cos\theta - S_{\mathrm{rej}\_c}(\theta) \times (1 - P_{\mathrm{c}}(\theta)) \times (\mathrm{j} - 1)}\right] \quad (13)$$

meet the spherical distribution, and $G(\theta)$ in the Eq. (4) is equal to 0.5. It is a common assumption in the field of remote sensing (Fan et al. 2014a, b; Nilson et al. 2011); and (3) $\Omega_{\mathrm{C}}(\theta)$ is assumed to equal to 1. These assumptions may be violated for specific trees in real forests, but they can clearly reveal how the exclusion distance affects GF and CI in forest plantations to avoid the influences of other factors.

Simulated data are used here, and the validation of the model is shown in the next section. RASD ranges from 0 to 1.14 in the simulations, and the other simulated input parameters are listed in Table 1. 1.14 is the largest allowable value of RASD in this simulated forest stand, because

$$S_{\mathrm{rej}\_c}(\theta) = \begin{cases} s_{\mathrm{crust}\_c}(\theta) & \text{for} \quad R_{\mathrm{ASD}} \le 1 \\ s_{\mathrm{crust}\_c}(\theta) - s_{\mathrm{pse}\_c}(\theta) & \text{for} \quad R_{\mathrm{ASD}} > 1 \quad \text{and} \quad (R_{\mathrm{ASD}} \times r) \times \cos(\theta) \ge t_{\mathrm{h}}(\theta) \\ t_{\mathrm{c}}(\theta) & \text{for} \quad x > r \quad \text{and} \quad x \times \cos(\theta) \ge t_{a\_b}(\theta) \end{cases} \quad (14)$$

where $t_{\mathrm{h}}(\theta)$ is one half of the projection of crowns height normal to θ; $S_{\mathrm{rej}\_c}(\theta)$ is the true repulsion area for calculating GF; $s_{\mathrm{crust}\_c}(\theta)$ represents the crust area of a crown and it can be calculated as

$$s_{\mathrm{crust}\_\mathrm{c}}(\theta) = (R_{\mathrm{ASD}} \times r)^2 \times \pi \times \cos(\theta) \quad (15)$$

$s_{\mathrm{pse}\_c}(\theta)$, which is inside of the crust but outside of the crown, is pseudo repulsion area of the crown (Fig. 3c).

Results

For the purpose of demonstrating the influences of exclusion distances on GF and CI, several assumptions are made here: (1) spheroids are chosen for crowns. In fact, there are infinite variety of shapes that spheroids can approximate (Norman, 1983); (2) inclinations of shoots are assumed to

crowns or crusts of crowns could beyond the borders of forest stand if RASD is greater than 1.14.

As shown in Fig. 4, the exclusion distances among trees have strong impacts on GF. The red line, which represents GF simulated by the Poisson model, is the maximum at any θ. The overall GF decreases progressively with increasing θ and RASD. The differences among the seven GF values vary with θ: the higher the value of θ, the greater the difference among them, i.e., GF with RASD = 1 is 32.4 % lower than the Poisson's GF at $\theta = 0°$. However, the latter is over 22 times greater than the former at $\theta = 80°$.

The line with RASD = 1 is an obvious boundary for all GF values in Fig. 4: if RASD $\le$1, the six GF values have very similar variation trends: (1) the higher the value of RASD, the lower the value of GF; (2) the differences among the six GF values increase with the value of RASD varying from 0 to 1 at any θ. It is because the crust area of a

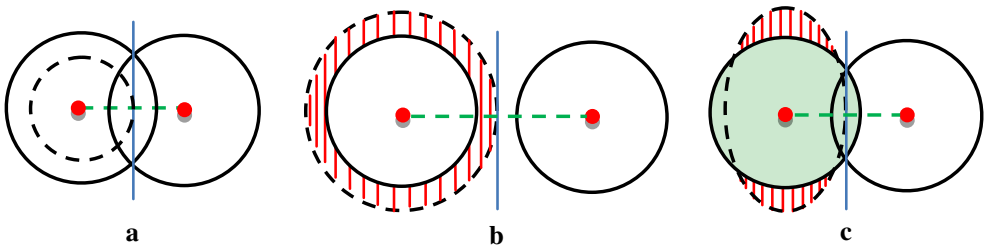

Fig. 3 Schematic of the hypergeometric model for trees in a forest plantation stand. *Solid circles* represent crowns; *green dash lines* represent the exclusion distances which are the products of RASD and the mean diameter of the crowns; *red zones* mean pseudo reject areas and need to be removed when calculating GF and CI. *Dash circles* are the "crusts" of trees. **a** The crust is *inside* of the crown if $\theta = 0$ and RASD <1; **b** the crust is *outside* of the crown if $\theta = 0$ and RASD >1; **c** if $\theta \neq 0$, the crust of the crown is not a *circle* but an *ellipse* (color figure online)

Table 1 Simulated model inputs

Parameters	Value
S (m^2)	100 × 100
N_c	2200
H_a (m)	1
H_b (m)	2
r	1
γ_e	1.33
LAI	5
Ω_C	1

In Table 1, H_a is the mean height of the lower part of the tree (trunk), H_b is the mean height of crowns, and r is the mean radius of crowns

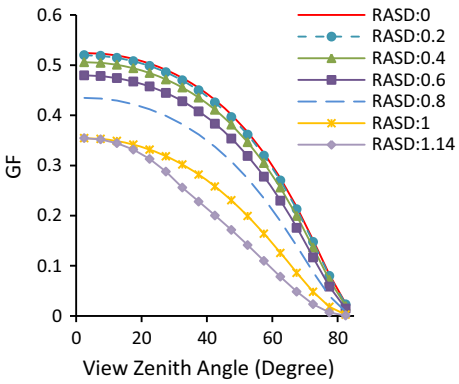

Fig. 4 Comparison of the GF of canopies with different RASD values

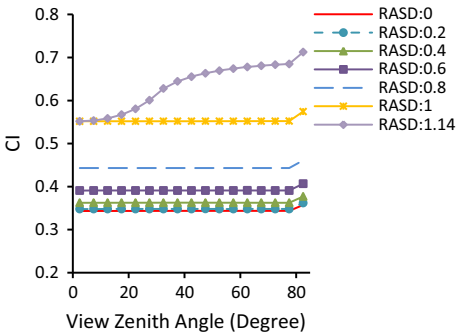

Fig. 5 Comparison of the CI of canopies with different RASD values

crown is linearly related to the square of RASD (Eq. 15). However, if RASD ≥1, the true repulsion area is not the total crust area of the crown, but the crust area subtracted by the pseudo repulsion area according to Eq. (14). If trees are assumed to be solid spheres, the total ground coverage of the spheres, which is equal to 1 − GF at $\theta = 0°$, is an invariant value; no matter how the spheres are distributed on the ground. Therefore, the two GF values with RASD ≥1 are nearly equal to each other at low θ. However, the crowns with RASD = 1 are more likely to overlap each other than the ones with RASD = 1.14 with increasing θ. In other words, the former distribute more regularly than the latter with increasing θ.

As shown in Fig. 5, the exclusion distances have also strong impacts on CI. The overall CI increases progressively with increasing RASD. Similarly, the line with RASD = 1 is also an obvious boundary. If RASD ≤1, six CI values have similar variation patterns: all CI values are almost the same at any θ (increase slightly at very large θ), and the differences among the six CI values increase with RASD varying from 0 to 1. However, CI increases quickly with increasing θ if RASD >1.

The maximum CI (about 0.7) in Fig. 5 is still smaller than 1. This means that leaves in the canopy are still clumped. It is due to that crowns form many clumped aggregations in the forest although the trees or crowns are regularly distributed in the forests and shoots are assumed to be randomly distributed within every crown.

In general, the exclusion distances have strong impacts on GF and CI: the larger the exclusion distance among trees, the more regular distribution of leaves in the canopy is; the greater the value of RASD, the lower the value of GF and the greater the value of CI.

Experimental validation

Pinus massoniana and *Populus davidiana*, which are two popular forest plantation tree species in China, were chosen to validate GF and CI calculated by the hypergeometric model. Two *P. massoniana* plantation stands (32°33′00″N, 118°12′09″E; 32°33′54″N, 118°12′14″E) and two *P. davidiana* plantation stands were chosen (32°29′05″N, 118°12′48″E; 32°30′59″N, 118°12′53″E). The two *P. massoniana* stands were about 30 years old (PM1) and 15 years old (PM2), respectively; the two *P. davidiana* stands were about 11 years old (PD1) and 8 years old (PD2), respectively. Four sample areas were all 100 × 100 m^2. The size, the number of crowns and the RASD of the stands were measured, respectively; needle-to-shoot area ratios were measured for the two coniferous forests (PM1 and PM2) and were equal to 1 for the two broad-leaved forests (PD1 and PD2); LAI were measured by destructive sampling: five representative trees were chosen first and then five representative branches were sampled from top to bottom of each tree; The mean angles between branches and trunks (α_{bj}), the mean angles between branches and twigs (α_{bbj}), as well as the mean angles between leaves or shoots and twigs (α_{Lj}) were measured. All needles or leaves on the sampled branches were collected. The lengths of the needles were measured; the radii of needles in an individual tree were assumed to be invariant. All leaves on the sampled branches of two broad-leaved

Table 2 Parameters of four sample plots

Parameters	PM1	PM2	PD1	PD2
H_a (m)	3.80	1.50	3.50	2.80
H_b (m)	6.40	2.1	7.10	5.90
r (m)	2.60	0.95	1.70	1.50
γ_e	1.70	1.75	1	1
N_c	420	1550	1020	890
RASD	0.85	1.05	0.90	1.12
LAI	4.30	3.20	4.80	3.10
α_{bj} (°)	65	70	15	20
α_{bbj} (°)	65	70	15	20
α_{Lj} (°)	50	55	80	80

In Table 2, α_{bj} is the mean angle between the branches and the trunk, α_{bbj} is the mean angle between the twigs and the branches, α_{Lj} is the mean angle between the leaves or shoots and the twigs

forests were laid on the ground one by one, and total leaf areas were measured using a digital camera. Finally, LAI was calculated as half the total needle or leaves area per unit ground surface (Chen and Black 1992). All GF values were measured below the overstory on an overcast day using Li-Cor LAI-2000 Plant Canopy Analyzer (LAI-2000), and CI was measured using the optical instrument Tracing Radiation and Architecture of Canopies (TRAC) at $\theta \approx 46°$ on a sunny day in October 2013 in Chuzhou, China (Table 2).

If the inclination of leaves meets the conical distribution, the G value of leaves can be calculated by (Ross 1981; Leblanc et al. 1999):

$$G(\theta, \alpha_L) = \begin{cases} \cos\alpha_L \times \cos\theta & \theta \le \frac{\pi}{2} - \alpha_L \\ \cos\alpha_L \times \cos\theta \times \left[1 + 2 \times \frac{\tan x - x}{\pi}\right] & \theta > \frac{\pi}{2} - \alpha_L \end{cases} \quad (16)$$

where $x = \cos^{-1}(\cot\alpha_L \times \cot\theta)$ and α_L is the inclination angle of the leaves, and θ is the view or solar zenith angle.

However, forest canopies often have obvious hierarchical structures, i.e., branches and twigs, etc., and these structures have significance in the stand-level radiation transmission at various angles and therefore the overall G value of the stand. Leaves often incline to twigs rather than trunk or branches.

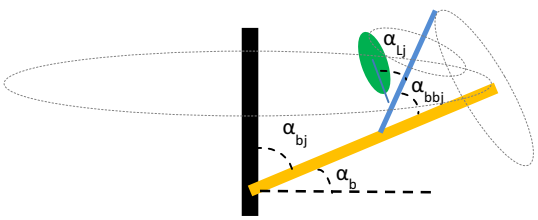

Fig. 6 Schematic diagram for the two trees species, where α_{bj} is the angle between branches and the tree trunk, α_{bbj} is the angle between a twig and a branch, α_{Lj} is the angle between a leaf and a twig. The dotted ovals represent the "children" structures round the "mother" structures

The inclinations of leaves in a branch or a twig are different for the two tree species because leaves are around every twig and twigs are around every branch (Fig. 6). While, in a branch level, the angles between the branch and twigs have no obvious differences; similar characteristics could be shown in a twig level where the angles between the twig and leaves also show little changes. In fact, many trees have these sub-crown characteristics. The assumption that the angles between "children" structures and "mother" structures within a crown (Fig. 6) have no obvious differences was often made in many plant structural models (Perttunen et al. 1996, 2001; Chen et al. 1994; Lacointe 2000). These growth patterns provide a means of calculating the overall G value for the canopy. In Eq. (16), two angles are defined: (1) the angle between the direction of view or light and the trunk (θ), and (2) the angle between the leaves and the trunk ($\pi/2 - \alpha_L$). These two angles are important to determine the overall G value. In this paper, the stand-level G value can be calculated similar to Eq. (16), but the vertical coordinate of spatial reference systems in Eq. (16) need to be rotated from the trunk to branches or twigs.

The light interception coefficient G of the canopy can be calculated as

$$G(\theta_{sbb}) = \frac{1}{4\pi^2} \int_0^{2\pi} \int_0^{2\pi} G_0\left(\theta_{sbb}, \pi/2 - \alpha_{Lj}\right) d\beta_{bb} d\beta_b \quad (17)$$

where θ_{sbb} is angle between light or view direction and a twig, and it can be calculated using the space geometry; $G_0\left(\theta_{sbb}, \pi/2 - \alpha_{Lj}\right)$ is the G value of leaves on a twig, and it can be calculated using Eq. (16). β_b is the azimuth angle of branches, and β_{bb} is the azimuth angle of twigs.

As shown in Fig. 7, GF values simulated by the hypergeometric model are closer to the measurements than those simulated by the Poisson model at most zenith angles for the four stands. The root mean squared error (RMSE) between the simulations of the hypergeometric model and the measurements at the first four zenith angles of LAI-2000 ($\theta = 7°$, 23°, 38° and 53°) for the four stands is about 0.036, 0.042, 0.037 and 0.041, respectively; while RMSE between the simulations of the Poisson model and the measurements at the first four zenith angles of LAI-2000 is about 0.108, 0.059, 0.128 and 0.140, respectively.

The measurements of GF are apparently lower than the simulations at the fifth ring of LAI-2000 ($\theta = 68°$). This is because of the tree trunks which had intercepted substantial parts of light at high θ but they are not considered in the simulations. All GF values simulated by the hypergeometric model are lower than the measurements at low θ, suggesting that the angular distributions of leaves, twigs and branches included in Eq. (17) may have not been sufficient to consider the stand-level G value. We postulate that the tree crown shape might have a role to play in this model

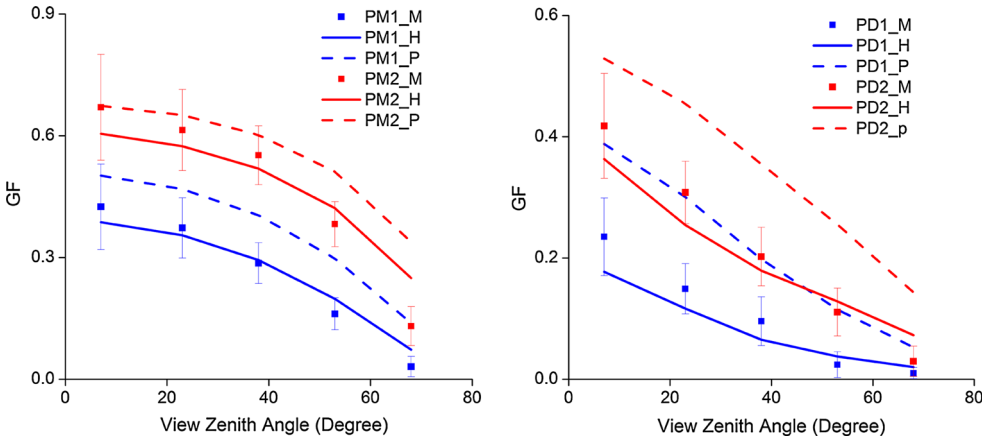

Fig. 7 Comparison of measurements and simulations of GF in the four forest plantation stands (Postfix "_M" means the measurements of GF; "_H" means GF simulated by the hypergeometric model; "_P" means GF simulated by the Poisson model)

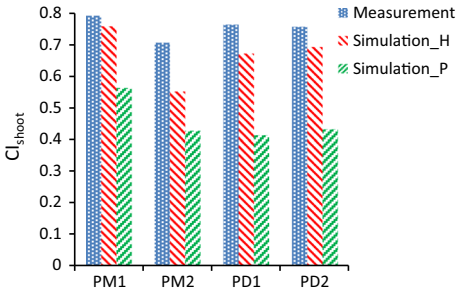

Fig. 8 Comparison of measurement of CI_{shoot} with simulations in the four stands (simulation_H are the CI_{shoot} simulated by the hypergeometric model; simulation_P are the CI_{shoot} simulated by the Poisson model)

underestimation of GF against measurements, because the vertical tree crown shape can induce larger GF values at lower zenith angles than our model assuming no tree crown geometrical effect. The assumption of the random distribution of leaves or shoots within the crowns may also cause error: leaves or shoots are in fact aggregated to some extent within the crowns because of the hierarchical characteristics of sub-crowns. However, we deem that the sub-crown structures are highly complex, and both clumped and regular distribution patterns of leaves or shoots may coexist within a crown. From the measurement of GF (Fig. 7), the clumping effects of leaves or shoots within the crowns are not obvious at $\theta \approx 40°$, especially for the PM1 stand where GF values simulated by the hypergeometric model agree well with the measurements at the first four zenith angles of LAI-2000.

The gaps within a shoot are so small that TRAC hardly detects them due to the penumbra effect (Chen and Cihlar 1995); therefore, CI measured by TRAC is in fact clumping index at scales larger than the shoot level (CI_{shoot}) (Chen and Cihlar 1995). The relationship between CI_{shoot} and CI is: $\Omega = \Omega_E/\gamma_e$, where Ω_E means CI_{shoot} (Chen 1996).

As shown in Fig. 8, there are no obvious differences between measurements and simulations of CI_{shoot} using the hypergeometric model for the PM1, PD1 and PD2 stands. However, the differences between measurements and simulations using the Poisson model are very significant for all the four stands. The measurements are distinctly larger than simulations used by the hypergeometric model for the PM2 stands because of the strong clumping effects within crowns.

Discussion

Clumping effects

The hypergeometric model is proposed for forest plantations at the stand level. The differences of tree distribution patterns in the forest among the Poisson model, the Neyman-A model and the hypergeometric model are studied in "Theory and methods". It is shown that the hypergeometric model is more suitable for describing the spatial relationship among trees in forest plantations at the stand level than the Poisson model and the Neyman-A model.

The differences in GF or CI between the Neyman-A model and the hypergeometric model are not given in this paper. In fact, GF values simulated by the Neyman-A model are even larger than those by the Poisson model, and therefore, they are much larger than those by the hypergeometric model. There are no obvious patches or clumps of trees in most forest plantations.

On a landscape with multiple forest plantations, individual plantations may be regarded as forest patches, and clumping of trees may occur at scales larger than the stand level. In this case, the tree spatial distribution at the landscape level may be described using multiple hypergeometric models, where the hypergeometric model with different coefficients is used for the individual mosaics of the landscape.

In many natural forests, there are often different tree species with various crown sizes and clumped tree distributions. Therefore, the Neyman model is more suitable than the hypergeometric model for these natural forests. However, the Neyman model assumes a random

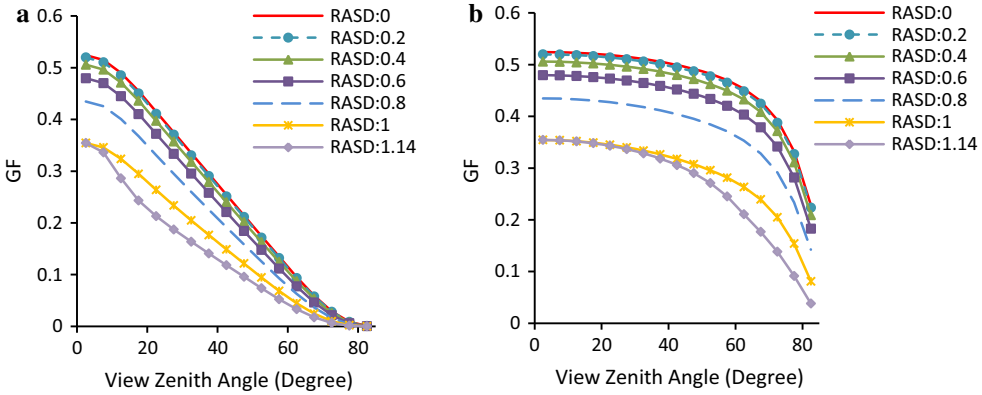

Fig. 9 Comparison of GF of two crown shapes with different RASD. **a** Prolate ellipsoids; **b** oblate ellipsoids. *Values in legend* represent the values of RASD

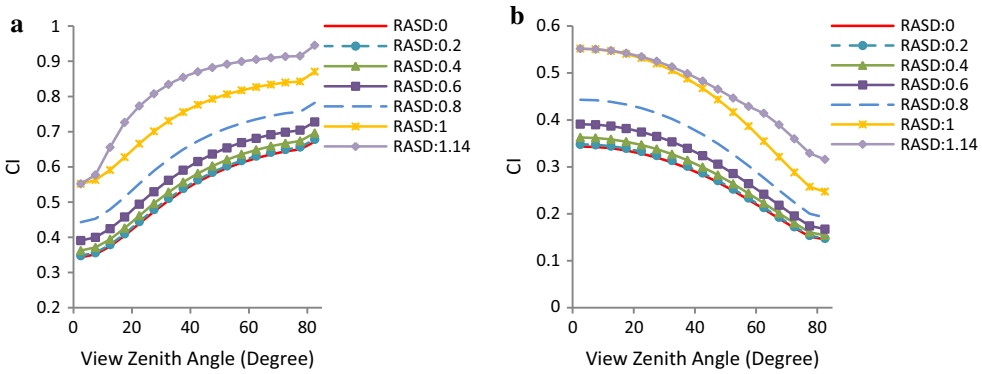

Fig. 10 Comparison of CI of two crown shapes with different RASD. **a** Prolate ellipsoids; **b** oblate ellipsoids. *Values in legend* represent the values of RASD

spatial distribution of tree groups and a random spatial distribution of trees within each group. It is therefore incapable of simulating the mutual repulsion among trees in competition of light and other resources. The mathematical treatment of this repulsion effect developed for the hypergeometric model would have implications on the further development of the Neyman model to consider this repulsion effect. For natural stands, where tree groups are distinctly or regularly distributed, the hypergeometric model may also be applicable, and more research can be conducted to demonstrate this applicability. For natural stands, where trees are randomly distributed, the hypergeometric model can be used as the Poisson model (special case) to describe the tree distribution.

Crown shapes

For convenience, the simulated crowns in "Results" are assumed to be spherical; however, spheroid is an ideal crown shape. Prolate and oblate ellipsoids are discussed here. The radius of the two types of ellipsoids is also equal to the horizontal radius of spheroids, but the height of prolate and oblate ellipsoids is three times and one third of the height of spheroids, respectively.

Figure 9 shows very similar variations to Fig. 4: the GF values decrease with increasing θ; the larger the value of RASD, the lower the value of GF. The line with RASD $= 1$ is also a boundary. A notable difference from the spheroid case is that GF changes quickly at low θ for prolate ellipsoids but at high θ for oblate ellipsoids. The CI values of three crown shapes are also all the same at $\theta = 0$ (Figs. 5, 10). However, the CI values are different among three crown shapes: the CI values of the spheroids are nearly all the same at any θ, while CI of prolate ellipsoids increases and CI of oblate ellipsoids decreases with increasing θ. This is because GF in an individual crown is the same at any θ for spheroids but changes for prolate or oblate ellipsoids with increasing θ.

Conclusion

Plantations are forests created by man, by planting seeds or seedlings. The human influence gives rise to larger exclusion distances among trees in forest plantations than those

in natural forests. Therefore, previous tree distribution models commonly used for natural forests (the Poisson model and the Neyman-A model) are not suitable for forest plantations. Through developing a hypergeometric model for describing tree distributions in forest plantations and validation of the model using measurements in four forest plantations, the following conclusions are drawn:

1. A simple and general distance factor defined as relative allowable shortest distance between centers of two adjacent crowns divided by the mean diameter of the crowns (RASD) is proposed to describe quantitatively the degree of mutual exclusion among trees at the stand level for forest plantations of various tree distribution patterns.
2. The hypergeometric model is more suitable than the Poisson model and Neyman-A model for describing the topological relationship among trees in forest plantations, which have the tendency towards regular tree distribution patterns. The Poisson model is a special case of the hypergeometric model for describing trees distribution, and it can be replaced by the hypergeometric model.
3. The exclusion distance has strong impacts on gap fraction (GF) and clumping index (CI) at the stand level for forest plantations. The results show that the exclusion among trees induces the tendency of regular distributions of leaves or shoots in the canopy: the larger the exclusion distance among trees, the more regular distribution of leaves (greater CI) in the canopy is; the greater the value of RASD, the lower the value of GF is. This tendency occurs because of the clumping of foliage within crowns is partially compensated by the regular tree distribution patterns.

Author contribution statement Geng J, Chen JM and Tian QJ: designing the experiment; Geng J, Chen JM and Tu LL writing the paper; Geng J, Wang L, Yang RR, Yang YJ and Huang Y running the experiment, Fan WL, Lv CG and Zheng G: significantly useful discussion for the paper.

Acknowledgments This research was supported by the National Science and Technology Major Project (Grant Nos. Y20A-C04 and Y20A-D52, in China), National Program on Key Basic Research Project of China (Grant Nos. 03-Y20A04-9001-15/16 and 30-Y20A29-9003-15/17), National Science Foundation of China (Grant Nos. 41401418/D0106). The authors are grateful to Shaojie Sun, Hongwei Wei, Yan Wang, Nianxu Xu, Nan Xia et al. for assistance with field work, Yongkang Feng and Professor Ju Weimin et al. for paper discussion. The core codes of the hypergeometric model would be available upon a request.

Compliance with ethical standards

Conflict of interest The authors declare that they have no conflict of interest.

References

Chen JM (1996) Optically-based methods for measuring seasonal variation of leaf area index in boreal conifer stands. Agric For Meteorol 80:135–163

Chen JM, Black TA (1992) Defining leaf area index for non-flat leaves. Plant Cell Environ 15:421–429

Chen JM, Cihlar J (1995) Plant canopy gap-size analysis theory for improving optical measurements of leaf-area index. Appl Opt 34:6211–6222

Chen JM, Leblanc SG (1997) A four-scale bidirectional reflectance model based on canopy architecture. Geosci Remote Sens IEEE Trans Geosci Remote Sens 35:1316–1337

Chen SG, Ceulemans R, Impens I (1994) A fractal-based Populus canopy structure model for the calculation of light interception. For Ecol Manag 69:97–110

Chen JM, Liu J, Cihlar J, Goulden ML (1999) Daily canopy photosynthesis model through temporal and spatial scaling for remote sensing applications. Ecol Model 124:99–119

Chen JM, Menges CH, Leblanc SG (2005) Global mapping of foliage clumping index using multi-angular satellite data. Remote Sens Environ 97:447–457

Da Silva D, Han L, Costes E (2014) Light interception efficiency of apple trees: a multiscale computational study based on MAppleT. Ecol Model 290:45–53

Demarez VER, Duthoit S, Baret FEDE, Weiss M, Dedieu GER (2008) Estimation of leaf area and clumping indexes of crops with hemispherical photographs. Agric For Meteorol 148:644–655

Duursma RA, Makela A (2007) Summary models for light interception and light-use efficiency of non-homogeneous canopies. Tree Physiol 27:859–870

Duursma RA, Falster DS, Valladares F, Sterck FJ, Pearcy RW, Lusk CH, Sendall KM, Nordenstahl M, Houter NC, Atwell BJ, Kelly N, Kelly J, Liberloo M, Tissue DT, Medlyn BE, Ellsworth DS (2012) Light interception efficiency explained by two simple variables: a test using a diversity of small- to medium-sized woody plants. New Phytol 193:397–408

Fan W, Chen JM, Ju W, Nesbitt N (2014a) Hybrid geometric optical-radiative transfer model suitable for forests on slopes. IEEE Trans Geosci Remote Sens 52:5579–5586

Fan W, Chen JM, Ju W, Zhu G (2014b) GOST: a geometric-optical model for sloping terrains. IEEE Trans Geosci Remote Sens 52:5469–5482

Franklin J, Michaelsen J, Strahler AH (1985) Spatial analysis of density dependent pattern in coniferous forest stands. Vegetatio 64:29–36

He L, Chen JM, Pisek J, Schaaf CB, Strahler AH (2012) Global clumping index map derived from the MODIS BRDF product. Remote Sens Environ 119:118–130

Iio A, Fukasawa H, Nose Y, Naramoto M, Mizunaga H, Kakubari Y (2009) Within-branch heterogeneity of the light environment and leaf temperature in a *Fagus crenata* crown and its significance for photosynthesis calculations. Trees 23:1053–1064

Lacointe A (2000) Carbon allocation among tree organs: a review of basic processes and representation in functional-structural tree models. Annals For Sci 57:521–533

Leblanc SG, Bicheron P, Chen JM, Leroy M, Cihlar J (1999) Investigation of directional reflectance in boreal forests with an improved four-scale model and airborne POLDER data. Geosci Remote Sens IEEE Trans Geosci Remote Sens 37:1396–1414

Lewis P, Disney M (2007) Spectral invariants and scattering across multiple scales from within-leaf to canopy. Remote Sens Environ 109:196–206

Li X, Strahler AH (1988) Modeling the gap probability of a discontinuous vegetation canopy. Geosci Remote Sens IEEE Trans Geosci Remote Sens 26:161–170

Massonnet C, Regnard JL, Lauri PE, Costes E, Sinoquet H (2008) Contributions of foliage distribution and leaf functions to light interception, transpiration and photosynthetic capacities in two apple cultivars at branch and tree scales. Tree Physiol 28:665–678

Mottus M, Sulev M, Lang M (2006) Estimation of crown volume for a geometric radiation model from detailed measurements of tree structure. Ecol Model 198:506–514

Munier-Jolain NM, Guyot SHM, Colbach N (2013) A 3D model for light interception in heterogeneous crop:weed canopies: model structure and evaluation. Ecol Model 250:101–110

Nelson AS, Weiskittel AR, Wagner RG (2014) Development of branch, crown, and vertical distribution leaf area models for contrasting hardwood species in Maine, USA. Trees 28:17–30

Neyman J (1939) On a new class of "Contagious" distributions, applicable in entomology and bacteriology. Ann Math Stat 10:35–57

Niinemets Ü (2010) A review of light interception in plant stands from leaf to canopy in different plant functional types and in species with varying shade tolerance. Ecol Res 25:693–714

Nilson T (1971) A theoretical analysis of the frequency of gaps in plant stands. Agric Meteorol 8:25–38

Nilson T, Kuusk A, Lang M, Pisek J, Kodar A (2011) Simulation of statistical characteristics of gap distribution in forest stands. Agric For Meteorol 151:895–905

Norman JM (1983) Radiative transfer in an array of canopies. Agron J 75:481

Perttunen J, Sievanen R, Nikinmaa E, Salminen H, Saarenmaa H, Vakeva J (1996) LIGNUM: a tree model based on simple structural units. Ann Bot 77:87–98

Perttunen J, Nikinmaa E, Lechowicz MJ, Sievanen R, Messier C (2001) Application of the functional-structural tree model LIGNUM to sugar maple saplings (*Acer saccharum* Marsh) growing in forest gaps. Ann Bot 88:471–481

Ross J (1981) The radiation regime and architecture of plant stands. Dr W Junk, The Hague, p 9

Russell G, Jarvis PG, Monteith JL (1989) Plant canopies: their growth, form and function. Cambridge University Press, Cambridge, p 178

Sinoquet H, Stephan J, Sonohat G, Lauri PE, Monney P (2007) Simple equations to estimate light interception by isolated trees from canopy structure features: assessment with three-dimensional digitized apple trees. New Phytol 175:94–106

Talbot G, Dupraz C (2012) Simple models for light competition within agroforestry discontinuous tree stands: are leaf clumpiness and light interception by woody parts relevant factors? Agrofor Syst 84:101–116

West PW (2006) Growing plantation forests. Springer, Berlin, pp 9–25

Xue BL, Kumagai T, Iida S, Nakai T, Matsumoto K, Komatsu H, Otsuki K, Ohta T (2011) Influences of canopy structure and physiological traits on flux partitioning between understory and overstory in an eastern Siberian boreal larch forest. Ecol Model 222:1479–1490

Yang X, Yan E, Chang SX, Da L, Wang X (2015) Tree architecture varies with forest succession in evergreen broad-leaved forests in Eastern China. Trees 29:43–57

Zheng G, Moskal LM, Kim S (2013) Retrieval of effective leaf area index in heterogeneous forests with terrestrial laser scanning. IEEE Trans Geosci Remote Sens 51:777–786